

Meta-Reinforcement Learning for Universal Quadrupedal Locomotion Control

Fabrizio Di Giuro¹, Fatemeh Zargarbashi², Jin Cheng², Dongho Kang², Bhavya Sukhija² and Stelian Coros²

Abstract—This work presents a deep reinforcement learning-based approach to develop a policy for robot-agnostic locomotion control. Our method involves training an agent equipped with memory, implemented as a recurrent policy, on a diverse set of procedurally generated quadruped robots. We demonstrate that the policies trained by our framework transfer seamlessly to both simulated and real-world quadrupeds not encountered during training, maintaining high-quality motion across platforms. Through a series of simulation and hardware experiments, we highlight the critical role of the recurrent unit in enabling generalization, rapid adaptation to changes in the robot’s dynamic properties, and sample efficiency.

I. INTRODUCTION

While recent advances in reinforcement learning (RL) have demonstrated state-of-the-art performance in quadrupedal locomotion [1, 2, 3, 4, 5], typical RL-based methods train a control policy tailored to a specific robot embodiment. This requires retraining the policy whenever the robot’s morphological or dynamic properties change. This limitation hampers the applicability of these methods, as training a policy for a new morphology often necessitates additional reward or hyperparameter tuning.

In response, developing a robot-agnostic RL policy has recently gained attention. However, research efforts in this area [6, 7] have employed methods that require exposure to a plethora of different robots during training or an additional system identification module, which increases the complexity of the training and deployment process.

In this work, we aim to develop a robot-agnostic RL policy with generalization properties that enable *zero-shot* transfer to diverse legged robotic platforms with varying physical properties, which we refer to as *universal locomotion control* in this paper. Additionally, we seek to achieve sample efficiency by exposing the agent to only a limited number of robots during training, to enhance the practicality of the method. To this end, we leverage *working-memory meta-reinforcement learning* (meta-RL) [8, 9, 10, 11], which provides rapid adaptability and significant improvements in sample efficiency. Following this paradigm, our approach involves training a recurrent policy on a diverse set of

This manuscript is submitted and approved as a Master’s Thesis, as required for the fulfillment of the Master of Science in Robotics, Systems, and Control at ETH Zurich.

¹Fabrizio Di Giuro, the author is with the Department of Mechanical and Process Engineering (D-MAVT), ETH Zurich, Switzerland. fdigiuro@student.ethz.ch

²The supervisors of this project are with the Computational Robotics Lab in the Institute for Intelligent Interactive Systems (IIS), ETH Zurich, Switzerland. {fzargarbashi, jicheng, kangd, sukhijab, scoros}@ethz.ch

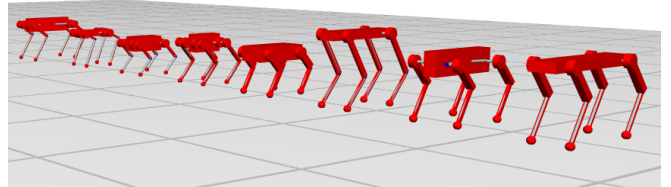


Fig. 1: Example of quadrupeds procedurally generated by randomizing the kinematic and dynamic parameters of *Unitree Go1* and *Unitree Aliengo*.

quadrupedal robots, each with its own morphological and dynamic parameters.

We provide experimental results in simulation to showcase the generalizability of our method. These results highlight the advantages of integrating meta-RL and offer insights into how various design choices affect the performance of the proposed framework. Additionally, through hardware experiments, we show that the policy synthesized with our method achieves zero-shot transfer to three quadrupedal robots, *Unitree Go1*, *Go2* and *Aliengo*, with different kinematic and physical properties.

II. RELATED WORK

A. Reinforcement Learning for Legged Locomotion

In recent years, RL has made significant strides in the field of legged locomotion. Unlike modular controller design complemented with model-based optimal control (MBOC) methods [12, 13, 14], which require carefully designed system models and simplifying assumptions, RL automates a substantial portion of the manual effort and design choices in developing locomotion controllers.

Pioneering efforts in applying RL to quadrupedal locomotion have successfully obtained robust locomotion controllers over rough [1, 2, 3] and deformable [5] terrains, often leveraging a student-teacher learning paradigm. One notable approach proposed by Peng et al. [15], known as *motion imitation*, enables physically simulated legged systems to learn realistic movement by imitating expert demonstrations, such as motion clips recorded from animals [16]. Building upon this, Kang et al. [4] proposed a framework that imitates on-demand MBOC demonstrations as reference motions.

Many RL-based methods rely on the *sim-to-real transfer* approach, which trains RL policies using trial-and-error data generated in physically simulated environments. This approach requires special measures to bridge the reality gap—the discrepancies that arise when transferring agents trained

in simulation to the real world. One approach to address this issue is to enhance the fidelity of the physical simulator by performing system identification from data collected on the real robot [1, 17]. Another widely adopted strategy is domain randomization, a technique that mitigates the mismatch between simulated and real-world environments by varying the physical parameters of the simulation during training [1, 16, 18, 19].

In our method, we adopt the reference-matching reward structure proposed by Kang et al. [4], as it allows the agent to learn user-desired behavior with minimal reward shaping. Instead of using MBOC demonstrations, we train an RL policy to match the robots’ state with kinematic motion references. To streamline sim-to-real transfer, we also apply the domain randomization technique, randomizing various physical parameters, including terrain friction coefficient and actuator latency.

B. Universal Locomotion Control

To achieve universal locomotion control, several efforts leverage modular robot design spaces by integrating morphology into a policy architecture to generalize motion across different robots with varying action and state spaces. For instance, Wang et al. [20] and Huang et al. [21] represent policies as Graph Neural Networks (GNNs), enabling decentralized control with centralized coordination. Alternatively, concurrent works utilize a Transformers architecture for the policy, conditioned on the agent’s morphology [22, 23, 24]. GNNs and Transformers have high computational demands. As a result, they have only been validated on planar simulated agents and lack real-world demonstration.

From a slightly different perspective, universal control is often framed as a multi-task RL (MTRL) problem, where the goal is to learn a contextual policy conditioned on a vector representation of the robot hardware [25, 26, 27]. This approach is often complemented with a separate module that performs adaptive system identification [26, 27], which was later applied to quadrupedal locomotion and demonstrated on multiple robot platforms by Luo et al. [7]. Meanwhile, Feng et al. [6] employ a fully connected architecture that uses a history of states and actions as input. This allows the network to learn the direct mapping from the history to suitable actions for a given embodiment, inferring the robot’s kinematic and dynamic properties via back-propagation.

Universal locomotion control can also leverage meta-RL algorithms. Belmonte-Baeza et al. [28] adopt Model-Agnostic Meta Learning [29] to train a locomotion policy. In this approach, a meta-policy is learned with a small number of trial-and-error data samples, and then fine-tuned for deployment on each robot embodiment.

In our method, we frame universal locomotion control as a working-memory meta-RL problem. Unlike the approach by Feng et al. [6], we generate a relatively small number (32) of robot morphologies using an unconstrained morphology randomization algorithm to reduce training time and enhance the practicality of the method. We then train a recurrent

policy across the generated morphologies using a model-free RL algorithm. Instead of providing the robot’s kinematic and physical properties as input to the policy [28], we use a Gated Recurrent Unit (GRU) [30] cell that learns to deduce this information online by updating its hidden state based on the agent’s experience in the environment.

III. PRELIMINARIES

A. Reinforcement Learning

RL is a subfield of machine learning where an agent learns to make sequential decisions through interaction with an environment to maximize cumulative rewards. At every step of interaction t , the agent receives the current state s_t from the environment, decides on an action a_t , observes the next state s_{t+1} and a scalar reward r_t , computed by the environment according to a dynamics function $P(s_{t+1}|s_t, a_t)$ and a reward function $R(s_t, a_t)$. The agent’s objective is to learn a policy π_θ that maps states to actions and maximizes the expected sum of discounted rewards over time:

$$J(\pi_\theta) = \mathbb{E}_\tau \left[\sum_{t=0}^H \gamma^t r(s_t, a_t) \right]. \quad (1)$$

Here, $\tau = (s_0, a_0, \dots)$ denotes the entire trajectory over the horizon H , where s_0 is sampled from the initial state distribution $\rho_0(s_0)$, $a_t \sim \pi_\theta(a_t|s_t)$, and $s_{t+1} \sim P(s_{t+1}|s_t, a_t)$.

B. Meta-Learning and Meta-RL

Meta-learning, or *learning-to-learn* focuses on developing algorithms that enable models to learn efficiently from experience [31]. Unlike traditional machine learning, where a model is trained on a fixed dataset for a specific task, meta-learning aims to train a model to generalize from a set of tasks $\mathcal{T}_{train} = \{\mathcal{T}_1, \mathcal{T}_2, \dots, \mathcal{T}_{N_{train}}\}$ so that it can quickly adapt to unseen, similar tasks $\mathcal{T}_{test} = \{\mathcal{T}_1, \mathcal{T}_2, \dots, \mathcal{T}_{N_{test}}\}$ with minimal or no fine-tuning. To enable generalization, it is crucial that the meta-training and meta-testing tasks share some structure, expressed by the assumption that they are samples drawn independently and identically from the same distribution, i.e. $\mathcal{T}_{train}, \mathcal{T}_{test} \sim \mathcal{T}$.

Meta-RL extends meta-learning principles to RL, where each task is a Markov Decision Process (MDP), i.e. $\mathcal{T}_i = \{S_i, A_i, P_i(s_{t+1}|s_t, a_t), R_i(s_t, a_t), \rho_{0,i}, \gamma, H\}$. In our problem formulation, \mathcal{T}_i represents a motion imitation task for a quadruped with embodiment i . Here, all tasks share the state and action space, and the reward function, but they differ in dynamics P_i and initial state distribution $\rho_{0,i}$. Meta-RL is akin to conducting RL in a Partially Observable MDP (POMDP) \mathcal{T}_i , where the agent learns a contextual policy conditioned on a context vector, $\pi_\theta(a_t|s_t, \phi_i)$. Unlike multi-task RL, the context ϕ_i in meta-RL is unknown, and the agent infers it from its experience in the environment \mathcal{T}_i . By exposing the agent to multiple environments during meta-training, we learn a policy which is contextually aware and capable of generalizing across similar environments [32].

Expanding on the concept of the meta-learner as a contextual policy, a natural architectural choice is an RNN, which

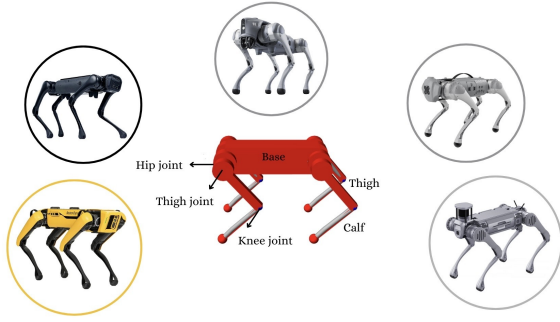


Fig. 2: Morphological template of most commercial quadrupedal robots. From left to right: *Boston Dynamics Spot* [34], *Unitree Aliengo* [35], *Unitree Go2* [36], *Unitree Go1* [37], *Unitree B2* [38].

ingests a history of states, actions, and rewards, encoding this information in its hidden state h_t . This method, known as working memory meta-RL, was introduced concurrently by Duan et al. [8] and Wang et al. [9]. These studies demonstrated that an RNN trained on interrelated environments with a model-free RL algorithm can implement a new RL algorithm through its recurrent dynamics. The rationale behind the use of RNNs is that learning can occur within new environments even if the network weights are frozen, as previously evidenced by Hochreiter et al. [33].

However, working-memory meta-RL has largely been confined to simulation due to practical challenges. Specifically, including the previous reward in input to the policy complicates hardware deployment. In our motion imitation formulation, computing the reward during hardware deployment would necessitate a reference, which, in turn, requires knowledge of the robot’s kinematic and dynamic parameters. This conflicts with our goal of achieving quadruped-agnostic control, hence we decided not to feed the reward in input to our policies. Moreover, we adopt the meta-episodic setting proposed by Duan et al. [8], which preserves the hidden state across K episodes of interaction with an environment. This setting encourages the recurrent agent to automatically learn exploration and perform well within the first K episodes of interaction with a new environment.

IV. METHOD

A. Morphology Generation

Commercially available quadrupedal robots typically follow a design template (see Fig. 2) comprising an unactuated base and four 3-DOF legs. Each leg is composed of a hip, a thigh, and a calf link, terminating in a point-foot. The three actuated joints in each leg are the hip abduction, hip extension, and knee extension joints, commonly referred to as the hip, thigh, and calf joints, respectively.

Given the morphology of a commercial robot, such as *Unitree Go1*, we generate a new morphology by updating the dimensions and mass properties of each link as illustrated in Fig. 3. For each link type (base, calf, thigh), we sample four scaling factors $[s_x, s_y, s_z, s_m]$ independently from a uniform distribution $U[0.5, 1.5]$. These scaling factors are applied linearly to the nominal dimensions $[l_x, l_y, l_z]$ and mass m

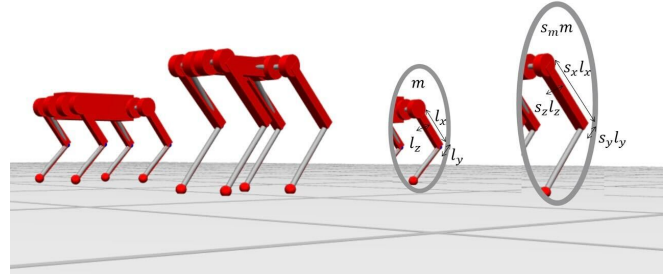


Fig. 3: Visualization of the morphology structure of *Unitree Go1* (on the left), and one of the morphologies generated according to our method (on the right). In the ovals, we highlight the properties of the thigh link of the hind-left leg.

of all instances of the link type, as follows:

$$\begin{bmatrix} l_{x,new} \\ l_{y,new} \\ l_{z,new} \\ m_{new} \end{bmatrix} = \begin{bmatrix} s_x & 0 & 0 & 0 \\ 0 & s_y & 0 & 0 \\ 0 & 0 & s_z & 0 \\ 0 & 0 & 0 & s_m \end{bmatrix} \begin{bmatrix} l_x \\ l_y \\ l_z \\ m \end{bmatrix}. \quad (2)$$

The matrix of inertia I of each link is recalculated by approximating the link with a cube and plugging the new mass and dimensions into the formula:

$$I = \begin{bmatrix} \frac{1}{12}m(l_y^2 + l_z^2) & m(l_x \cdot l_y) & m(l_x \cdot l_z) \\ m(l_y \cdot l_x) & \frac{1}{12}m(l_x^2 + l_z^2) & m(l_y \cdot l_z) \\ m(l_z \cdot l_x) & m(l_z \cdot l_y) & \frac{1}{12}m(l_x^2 + l_y^2) \end{bmatrix}. \quad (3)$$

We also modify the positions of each joint relative to the child and parent links accordingly. Additionally, we adjust the robot thigh joint angle in the initial configuration file to ensure that every foot lies below the corresponding hip joint, as required for stability and locomotion efficiency.

B. Overview of Framework

Our framework, illustrated in Fig. 4, creates a control policy that generates joint target positions based on the robot’s current state and high-level user commands, such as gait pattern and velocity command. It consists of three main components:

- A gait planner that translates the desired gait pattern into a contact timeline for each leg.
- A reference motion generator that produces reference trajectories for the base and feet, according to the body velocity command and the contact timeline.
- A policy network trained via motion imitation.

It is important to note that only the gait planner and the policy are deployed on the robot, making our control pipeline agnostic to the robot’s kinematic and dynamic parameters.

We formulate the motion imitation problem through RL by imitating on-demand reference motions, following the methodology proposed by Kang et al. [4]. However, instead of using a model-based optimal planner, we utilize a kinematics planner to generate reference base trajectories and footholds. This planner employs numerical integration and a straightforward foothold planning rule [39].

The observation of the policy o_t includes proprioceptive information, namely joint position q and speed \dot{q} , base height

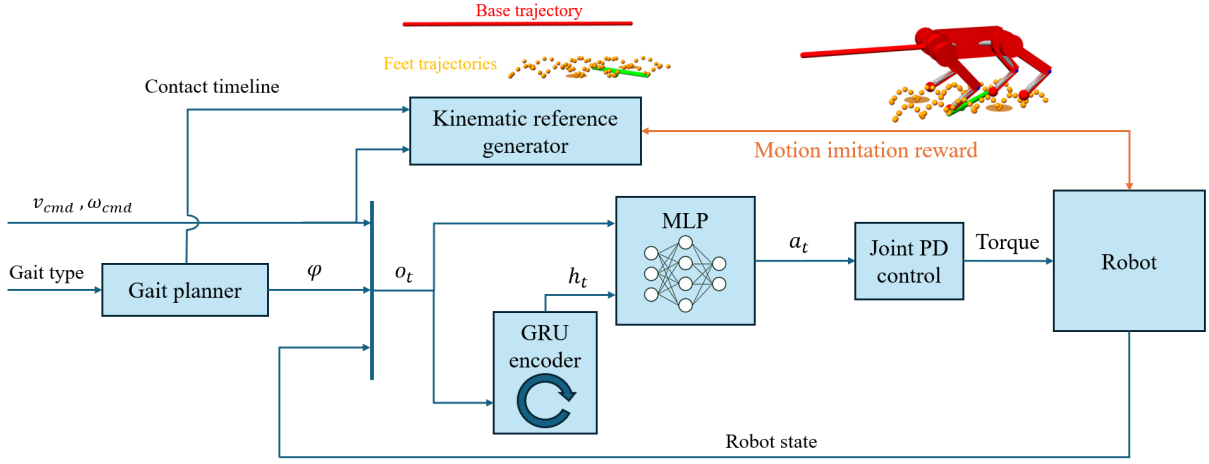


Fig. 4: Overview of our framework. The objective is to learn a universal policy that given joystick commands, maps the robot’s state (o_t) to target joint positions ($a_t = q_t^*$) for various quadruped designs. The policy is trained to maximise a reward that encourages tracking a reference motion, produced by a kinematic reference generator.

h , base linear velocity v and angular velocity ω , gravity vector g , as well as high-level navigation commands including forward velocity v_{cmd} , turning velocity ω_{cmd} , contact phase variables $\cos(\phi)$, $\sin(\phi)$, and finally, the previous action a_{t-1} . We use the contact phase parameterization proposed by Shao et al. [40], which represents a swing phase as $\phi \in [-\pi, 0)$ and a stance phase as $\phi \in [0, \pi)$.

The action a_t is the joint position targets, which are tracked by a PD controller with gains k_p and k_d .

Our reward function, inspired by Kang et al. [4], comprises an imitation term r^I and a regularization term r^R as

$$r = r^I \cdot r^R = (r^h \cdot r^v \cdot r^{ee} \cdot r^{\dot{\psi}}) \cdot (r^{\Delta a} \cdot r^{slip} \cdot r^{\theta_y, \theta_z}). \quad (4)$$

On the one hand, r^I encourages the alignment of base height $h \in \mathbb{R}$, velocity $v \in \mathbb{R}^3$, feet position $P_{ee} \in \mathbb{R}^{4 \times 3}$, and yaw rate $\dot{\psi} \in \mathbb{R}$ of the robot with the reference trajectories. On the other hand, r^R regulates action rate $\Delta a \in \mathbb{R}^{12}$, while minimizing contact feet velocity $v_{ee} \in \mathbb{R}^{4 \times 3}$, base pitch $\theta_y \in \mathbb{R}$ and roll $\theta_z \in \mathbb{R}$ angles. Each reward term maps the error between the reference x and the actual value \hat{x} to a scalar between 0 and 1 through the radial basis function kernel, with sensitivity σ_x :

$$r^x = \exp\left(-\left\|\frac{\hat{x} - x}{\sigma_x}\right\|^2\right). \quad (5)$$

At the start of each training episode, we randomly sample a velocity command and the initial robot state from one of the reference motions in the queue, according to the reference state initialization (RSI) approach proposed by Peng et al. [15]. We terminate an episode early if the robot collapses, i.e. if any part of the robot, apart from its feet, comes into contact with the ground.

C. Network Architectures and Training Setup

Our policy architecture comprises a GRU cell with a hidden state of size 32, which processes a sequence of observations of length 16. The hidden state h_t is concatenated with the current observation o_t and passed as input

Algorithm 1: Recurrent PPO

Input : Number of iterations N_{IT} , number of epochs N_E , number of minibatches N_M

Output: A control policy π_θ

Init. environment, π_θ , value network V_ϕ ;

Init. hyperparameters ϵ, γ ;

for $iteration=1, \dots, N_{IT}$ **do**

buff = [];

$\theta_{old} = \theta$;

Collect N rollouts using current policy;

Compute advantages \hat{A}_t using value function and rollout buffer;

for $epoch=1, \dots, N_E$ **do**

for $minibatch=1, \dots, N_M$ **do**

Sample sequences from buffer;

Compute surrogate objective L^{clip} ;

Update θ, ϕ using gradient descent;

end

end

end

return π_θ

to a multilayer perceptron (MLP) with two hidden layers of 256 units each and ELU activation function, followed by a linear output layer, as illustrated in Fig. 4. We employ a symmetric actor-critic setup, where both the actor and critic networks have access to the same information and share the same architecture, except for the linear output layer. However, these networks are separate and do not share weights. All control policies are trained using Proximal Policy Optimization (PPO) [41], in conjunction with General Advantage Estimation (GAE) [42].

For our recurrent policies, we employ a slight variation, which we call Recurrent PPO, where at each training step, fixed-length sequences of transitions are sampled from the rollout buffer, instead of single transitions (see Algorithm 1). Furthermore, following the meta-episodic framework pro-

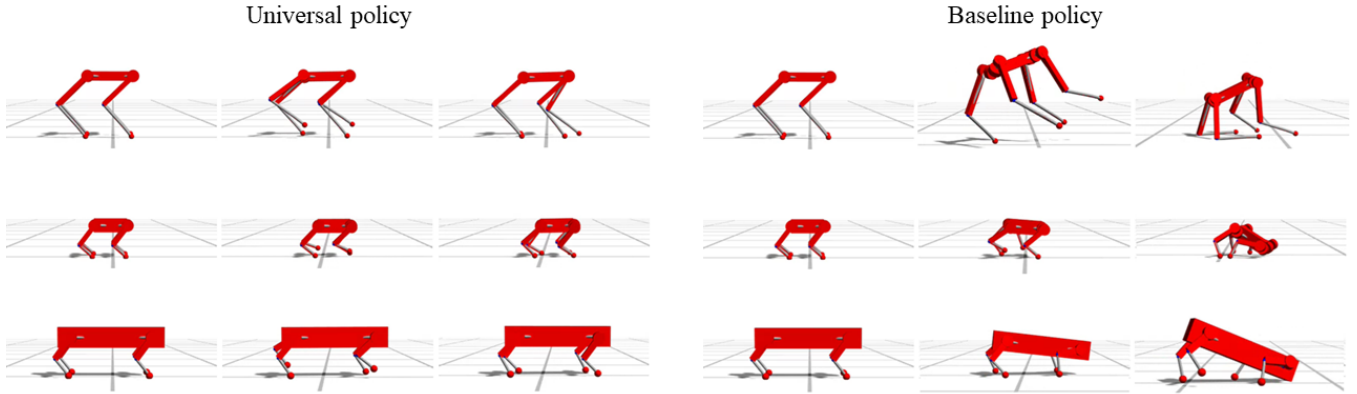


Fig. 5: Snapshots of three diverse simulated quadrupeds successfully trotting under our universal policy (left) and failing under a policy trained specifically for Unitree Go1 (right).

posed by Duan et al. [8], during rollout collection, the GRU hidden state is preserved across episodes, with a periodic reset every K episodes. This approach allows the agent to accumulate and leverage contextual information about the task structure and dynamics. Moreover, it enhances sample efficiency, as the agent makes more informed decisions based on the knowledge aggregated from multiple episodes.

Our policy is queried at a rate of 50 Hz, whereas the low-level PD controllers run at 200 Hz. Details of the reward parameters and training hyperparameters are provided in Table V and Table VI, respectively.

V. SIMULATION RESULTS

To evaluate the performance and robustness of our method, we conducted a series of comprehensive simulation experiments. All policies employed in the following experiments were trained using our proposed framework on a set of procedurally generated robots, as detailed in Section IV-A. To ensure a broad spectrum of training morphologies, we generated one half of the robot set by randomizing parameters of *Unitree Go1*, and the other half by randomizing parameters of *Unitree Aliengo*.

Each policy was trained to imitate a trotting gait reference with a gait cycle of 0.5 seconds, under varying velocity commands ranging from -0.5 m/s to 1.0 m/s. The training data was generated by our in-house physics simulator built on the Open Dynamics Engine (ODE) [43]. Additionally, to streamline the neural network training process, we normalized the observations using a running mean and standard deviation vector. We highlight all policies were trained for 163.84 million timesteps *without* dynamics randomization, except for exposure to the set of different embodiments.

A. Generalization over diverse embodiments

In our first simulation experiment, we demonstrate the efficacy of our framework in creating a universal control policy. Using our framework, we trained an RL policy, as detailed in Section IV. To highlight the effectiveness of our method, we also trained a baseline RL policy with a standard RL training setup without randomized embodiments¹ and

¹More specifically, we used *Unitree Go1* to train the baseline policy.

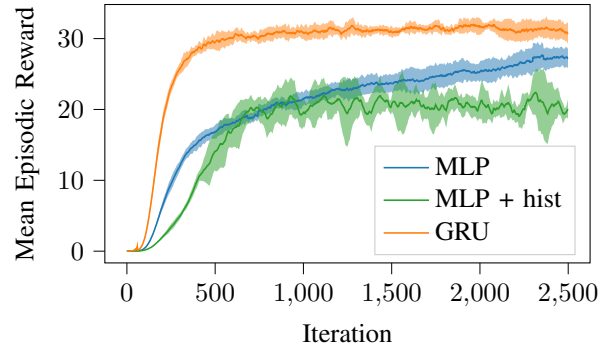


Fig. 6: Mean and standard deviation of reward curves during training for different architectures. The learning curves are smoothed with a moving average filter with window of 60 timesteps.

without GRU. We then assessed each policy on a population of simulated quadrupeds with diverse morphological and dynamic properties, that were *unseen* during the training.

Qualitative evaluations on a test set of 40 diverse robots demonstrated that our policy effectively generalized the trotting gait pattern, maintained the commanded speed, and achieved target values for base height and foot swing height as illustrated in Fig. 5. In contrast, the baseline policy failed to control unseen morphologies. This shows that universal locomotion control is achievable with our framework without extensive dynamics randomization, while the standard RL training procedure fails in this regard.

B. Comparison of Architectures

To demonstrate the critical role of the GRU encoder in our method, we compared our policy architecture against a fully connected architecture, henceforth denoted as MLP, consisting of two hidden layers of 256 units each, ELU activation function, and a linear output layer. As an additional baseline, we use another MLP, henceforth denoted as MLP + history, which takes as input a history of the last 16 observations. This architecture feeds the history through two hidden layers of size [1024, 512] with ELU activation function, similar to the architecture used by Feng et al. [6].

We trained 5 GRU policies, 5 MLP policies with the current observation only, and 5 MLP policies with a window of 16 past observations, each with a separate random seed.

TABLE I: Walk experiment: Mean Episodic Reward (MER)

v_{cmd} [m/s]	GRU	MLP + hist	MLP
$\{-0.1, 0.1\}$	103.761	95.480	99.160
$\{-0.2, 0.2\}$	99.520	89.564	95.886
$\{-0.3, 0.3\}$	92.162	81.708	90.764
$\{-0.4, 0.4\}$	83.048	72.413	82.610

TABLE II: Mass curriculum experiment: Mean Episodic Reward (MER)

s_m	GRU	MLP + hist	MLP
0.8	183.761	164.648	178.338
0.9	187.313	167.127	182.313
1.1	185.936	166.120	179.579
1.2	172.843	165.581	170.092

Each policy was trained on the same set of 32 robots. The training process took around 17, 20 and 28 hours on an NVIDIA GeForce RTX 2080 Ti (8 GB RAM) for MLP, MLP+history and GRU policies, respectively.

As depicted by the learning curves in Fig. 6, GRU networks attain a significantly higher final reward and show higher sample efficiency compared to other network architectures. Interestingly, providing a history of observations to the MLP does not improve the learning curve; rather, it tends to increase oscillations. We believe this could be mitigated with more thorough hyperparameter tuning, or with a deeper policy network.

We conducted two robustness tests across a test set of 40 simulated quadrupeds, not seen during training:

- The **walk test**, which involved walking for 4 seconds with symmetric commanded speeds $v_{cmd} = \{-x, x\}$ m/s, over a total of 2000 episodes.
- The **mass curriculum test**, which consisted in walking for 8 seconds with commanded speeds $v_{cmd} = \{-0.3, 0.3\}$ m/s, over a total of 2000 episodes. Every 2 seconds, the trunk mass was scaled abruptly by s_m .

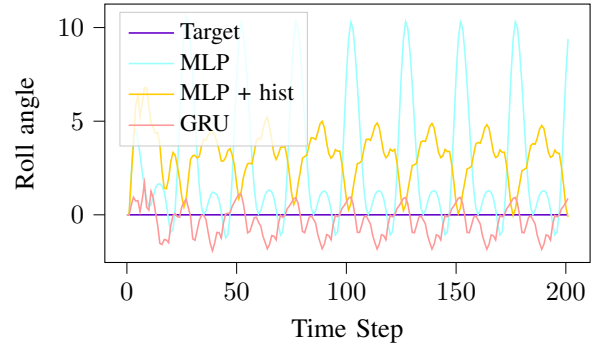
The Mean Episodic Reward (MER) served as the performance metric, computed as the average cumulative reward across all episodes:

$$MER = \frac{1}{N_{total}} \sum_{i=1}^{N_{total}} \left(\sum_{t=0}^H r_{i,t} \right). \quad (6)$$

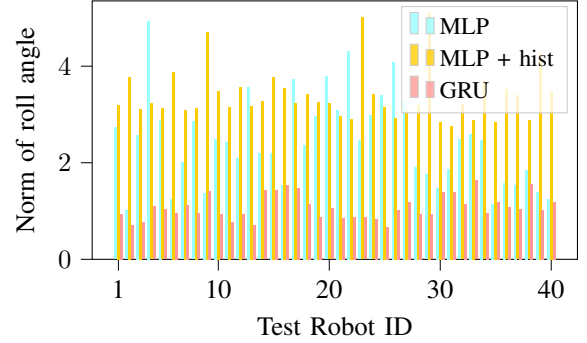
The results in Table I and Table II show that our GRU-based approach outperforms both MLP variants, underscoring the importance of the GRU encoder for generalizing to unseen robots and adapting to dynamic parameter variations.

Additionally, we visually compared the quality of the motion induced by different architectural choices and observed substantial differences, as detailed in the supplementary video. Notably, only the policy equipped with the recurrent unit demonstrated consistent and smooth motion, effectively maintaining the base roll angle close to the zero reference throughout the simulation. This behaviour is depicted in Fig. 7a, which shows the base roll angle trajectories for 4 seconds of walking on one of the test robots.

We complemented this insight with a quantitative analysis, to demonstrate the consistency of this behaviour across different quadrupeds.



(a) Evolution of roll angle θ_z [deg] for different architectural choices.



(b) L2-norm of roll angle $\|\theta_z\|$ [deg] for different architectural choices, across the test robots.

Fig. 7: Quality of motion experiment: base roll angle θ_z .

TABLE III: Walk experiment: average L2-norm of roll angle $\|\theta_z\|_{avg}$ [deg]

v_{cmd} [m/s]	GRU	MLP + hist	MLP
-0.5	1.405	3.872	2.357
-0.4	1.281	3.446	2.291
-0.3	1.223	3.397	2.249
-0.2	1.251	3.268	2.257
-0.1	1.144	3.209	2.247
0	1.282	3.316	2.272
0.1	1.122	3.268	2.349
0.2	1.076	3.397	2.447
0.3	1.090	3.850	2.554
0.4	1.402	4.149	3.194
0.5	1.357	4.326	2.867

Specifically, we computed the L2-norm of the base roll angle (θ_z in the form of YXZ Euler’s angles), over an episode of $H=200$ timesteps (4s) of walking:

$$\|\theta_z\| = \sqrt{\frac{1}{H} \sum_{t=0}^H \hat{\theta}_{z,t}^2}. \quad (7)$$

Fig. 7b compares $\|\theta_z\|$ for each robot, and Table III reports the average across the test set $\|\theta_z\|_{avg} = \frac{1}{N_{test}} \sum_{i=1}^{N_{test}} \|\theta_z\|_i$ for different speed commands. These results emphasize the outstanding performance achieved by the GRU policies.

C. Number of Training Robots

To evaluate the effect of the training set size, we trained 5 GRU policies with our method on a subset of 8 robots from the initial 32. The performance degradation with fewer training robots, in terms of Mean Episodic Reward (MER)

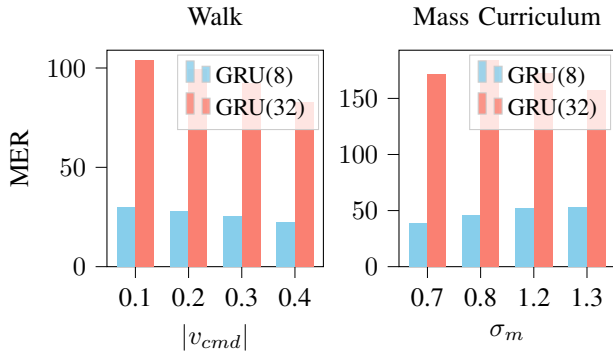


Fig. 8: Mean episodic reward (MER) achieved on walk and mass curriculum experiments from GRU policies trained on 32 and 8 robots.

achieved in the walk and mass curriculum tests, is summarized in Fig. 8. Policies trained on a smaller number of robots exhibit reduced generalization ability on the test set, and lower robustness to parameter changes, compared to those trained on the complete set. This suggests that both the number and diversity of robots encountered during training are crucial for the efficacy of our method.

In fact, training requires a sufficiently large and diverse set to enable generalization, but an excessively large training set may complicate optimizing for a universal policy. Consequently, our method benefits from a diverse and large enough training set, to enable the GRU encoder to capture the task distribution’s structure, thus facilitating generalization to unseen robots.

Additionally, we trained 5 MLP policies on the same 8 robots, demonstrating that the GRU module is essential for ensuring a higher degree of generalization from a smaller training set, as depicted in Fig. 9.

D. Meta-episode Length K

In another simulation experiment, we conducted an ablation study on the meta-episode length K , introduced by Duan et al. [8]. For each value of K we considered, we trained 5 policies with our method, each with a separate random seed. The learning curves in Fig. 10 reveal that lower values of K either result in a decreasing reward trend or in a very high variance between training runs. Conversely, preserving a multi-episodic memory (i.e. for $K > 2$) leads to stable training curves and higher final rewards. This study supports our earlier assertion that maintaining the GRU hidden state across episodes allows the agent to accumulate and leverage contextual information about the task structure and dynamics. Moreover, it demonstrates the sensitivity of our framework to the meta-episode length K , which appears to be a problem-dependent hyperparameter.

VI. HARDWARE RESULTS

To assess the effectiveness of the learned controller, we deployed it on three distinct commercial quadruped robots: *Go1*, *Go2*, and *Aliengo* from *Unitree*. Notably, the training robots were generated by randomly scaling the parameters of *Unitree Go1* and *Unitree Aliengo*, but the nominal parameters of the three quadrupeds were not specifically encountered during the training phase.

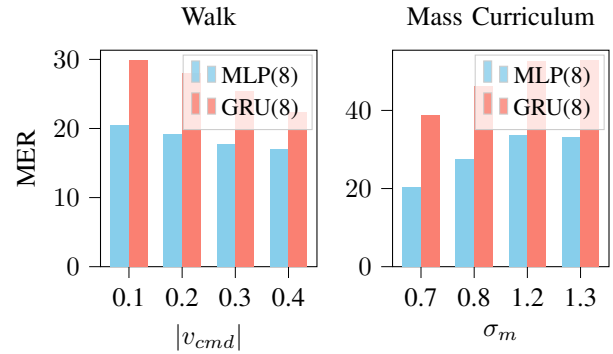


Fig. 9: Mean episodic reward (MER) achieved on walk and mass curriculum experiments from MLP and GRU policies trained on 8 robots.

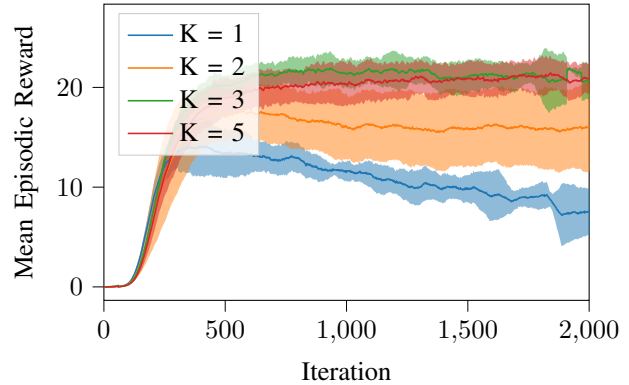


Fig. 10: Mean and standard deviation of reward curves during training for different meta-episode lengths K . The learning curves are smoothed with a moving average filter with window of 60 timesteps.

To ensure effective policy transfer to the hardware, we employed a Kalman filter-based state estimator, as described by Bledt et al. [44]. We introduced randomization in several dynamic parameters during training, in order to facilitate robust real-world performance. Specifically, we randomized the terrain friction coefficient, gravity vector g , and trained on uneven terrain generated using Perlin noise [2]. Additionally, noise was added to several observations during training, including joint position q and speed \dot{q} , base height h , base linear velocity v and angular velocity ω . We also incorporated impulse perturbations to enhance the policy’s resilience to external disturbances and randomized actuator delay to simulate latency. Table IV provides a comprehensive list of the randomized parameters and their respective ranges.

As demonstrated in the supplementary video and in Fig. 11, the universal policy trained with our method and extensive dynamics randomization successfully controlled locomotion across the three commercial quadrupeds. We attribute this success to the RNN’s ability to perform implicit system identification through its hidden state.

Furthermore, our hardware experiments underscored the necessity of extensive dynamics randomization during training to achieve successful sim-to-real transfer with recurrent policies. Our findings align with previous research by Siekmann et al. [45], which emphasizes the importance of comprehensive dynamics randomization to counteract the tendency of RNNs to overfit to simulation dynamics.

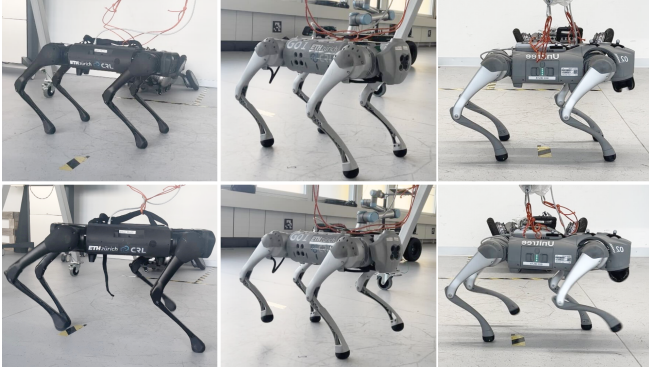


Fig. 11: Snapshots of the *Unitree Aliengo* (left), *Unitree Go1* (center) and *Unitree Go2* (right) successfully performing stand (top) and trot (bottom) motions, guided by our single universal policy.

TABLE IV: Parameters and their ranges used for hardware experiments

Parameter	Range
uneven terrain frequency	[0, 0.9]
uneven terrain height	[0, 0.1] m
friction coefficient	[0.5, 1.25]
projected gravity	[-1.70, 1.70] m/s ²
latency	[5, 40] ms
joint positions noise	[-0.01, 0.01] rad
joint velocity noise	[-1.5, 1.5] rad/s
base linear velocity noise	[-0.01, 0.01] m/s
base angular velocity noise	[-0.2, 0.2] rad/s
base height noise	[-0.05, 0.05] x nominal base height
linear velocity impulse	[-1.5, 1.5] m/s
angular velocity impulse	[-1.5, 1.5] rad/s

VII. CONCLUSIONS AND FUTURE WORK

In this work, we introduce a deep RL approach to train a universal locomotion controller for quadrupeds which enables zero-shot transfer to diverse legged robotic platforms with varying physical and kinematic properties. By leveraging the working-memory meta-RL paradigm, our method offers a straight-forward solution to the challenge of robot-agnostic locomotion control, while achieving higher sample efficiency compared to current existing methods.

In our simulation experiments, our method enabled generalization from a small number (32) of training robot morphologies. Furthermore, our hardware experiments demonstrate the capability of policies trained with our framework to achieve zero-shot transfer to three quadruped platforms, *Unitree Go1*, *Go2*, and *Aliengo*, despite these platforms not being seen during training.

The main limitation of our approach is its applicability primarily to robots sharing a morphological template with a 12 degrees of freedom. In the future, we aim to expand the applicability of our method to quadrupeds with different leg designs, such as the x-shaped designs or mechanically-coupled three-link leg designs. Moreover, we plan to explore more flexible policy architectures, to remove the constraint on the robot morphological template.

APPENDIX

Table V and Table VI provide reward coefficients and PPO hyperparameters used to train RL policies for the experiments presented in Section V and Section VI.

TABLE V: Reward hyperparameters

Reward term r^x	Sensitivity σ_x
base height r^h	0.05
base velocity* r^v	[0.3, 0.1, 0.3]
base yaw rate r^{ψ}	0.5
feet position* r^{ee}	[0.3, 0.05, 0.3]
action rate $r^{\Delta a}$	1.5
feet slip r^{SLIP}	0.1
pitch and roll $r^{\phi, \theta}$	0.5

* Non-scalar values are applied in forward-vertical-sideways order.

TABLE VI: PPO hyperparameters

Hyperparameter	Value
Batch size	512
Number of epochs	10
Value function coefficient	0.5
Entropy coefficient	0.01
Discount factor	0.95
Learning rate	5×10^{-5}
Episode length	128
Initial standard deviation	e^{-1}
Sequence length	16
Meta-episodic length	5

ACKNOWLEDGEMENT

Fabrizio Di Giuro expresses his heartfelt gratitude to his supervisors Fatemeh Zargarbashi, Jin Cheng, Dongho Kang, Bhavya Sukhija and Prof. Dr. Stelian Coros for their dedicated assistance and invaluable advice throughout the various stages of this research project. Their continuous support has made his initial research experience not only remarkably exciting, but also profoundly enriching. Additionally, Fabrizio extends his sincere thanks to Zijun Hui, Roberto Pellerito, and Francesco Ricca, for their insightful discussions during the course of this project.

REFERENCES

- [1] J. Hwangbo, J. Lee, A. Dosovitskiy, D. Bellicoso, V. Tsounis, V. Koltun, and M. Hutter, "Learning agile and dynamic motor skills for legged robots," *Science Robotics*, vol. 4, no. 26, p. eaau5872, 2019.
- [2] J. Lee, J. Hwangbo, L. Wellhausen, V. Koltun, and M. Hutter, "Learning quadrupedal locomotion over challenging terrain," *Science Robotics*, vol. 5, no. 47, p. eabc5986, 2020.
- [3] T. Miki, J. Lee, J. Hwangbo, L. Wellhausen, V. Koltun, and M. Hutter, "Learning robust perceptive locomotion for quadrupedal robots in the wild," *Science Robotics*, vol. 7, no. 62, p. eabk2822, 2022.
- [4] D. Kang, J. Cheng, M. Zamora, F. Zargarbashi, and S. Coros, "R1+ model-based control: Using on-demand optimal control to learn versatile legged locomotion," *IEEE Robotics and Automation Letters*, 2023.
- [5] S. Choi, G. Ji, J. Park, H. Kim, J. Mun, J. H. Lee, and J. Hwangbo, "Learning quadrupedal locomotion on deformable terrain," *Science Robotics*, vol. 8, no. 74, p. eade2256, 2023.
- [6] G. Feng, H. Zhang, Z. Li, X. B. Peng, B. Basireddy, L. Yue, Z. Song, L. Yang, Y. Liu, K. Sreenath *et al.*, "Genloco: Generalized locomotion controllers for quadrupedal robots," in *Conference on Robot Learning*. PMLR, 2023, pp. 1893–1903.
- [7] Z. Luo, Y. Dong, X. Li, R. Huang, Z. Shu, E. Xiao, and P. Lu, "Moral: Learning morphologically adaptive locomotion controller for quadrupedal robots on challenging terrains," *IEEE Robotics and Automation Letters*, 2024.
- [8] Y. Duan, J. Schulman, X. Chen, P. L. Bartlett, I. Sutskever, and P. Abbeel, "RL²: Fast reinforcement learning via slow reinforcement learning," *arXiv preprint arXiv:1611.02779*, 2016.
- [9] J. X. Wang, Z. Kurth-Nelson, D. Tirumala, H. Soyer, J. Z. Leibo, R. Munos, C. Blundell, D. Kumaran, and M. Botvinick, "Learning to reinforcement learn," *arXiv preprint arXiv:1611.05763*, 2016.
- [10] Y. Duan, *Meta learning for control*. University of California, Berkeley, 2017.
- [11] K. Rakelly, A. Zhou, C. Finn, S. Levine, and D. Quillen, "Efficient off-policy meta-reinforcement learning via probabilistic context variables,"

- in *International Conference on Machine Learning*. PMLR, 2019, pp. 5331–5340.
- [12] M. Kalakrishnan, J. Buchli, P. Pastor, M. Mistry, and S. Schaal, “Fast, robust quadruped locomotion over challenging terrain,” in *2010 IEEE International Conference on Robotics and Automation*. IEEE, 2010, pp. 2665–2670.
- [13] C. D. Bellicoso, F. Jenelten, C. Gehring, and M. Hutter, “Dynamic locomotion through online nonlinear motion optimization for quadrupedal robots,” *IEEE Robotics and Automation Letters*, vol. 3, no. 3, pp. 2261–2268, 2018.
- [14] D. Kang, F. De Vincenti, and S. Coros, “Nonlinear model predictive control for quadrupedal locomotion using second-order sensitivity analysis,” 2022.
- [15] X. B. Peng, P. Abbeel, S. Levine, and M. Van de Panne, “Deepmimic: Example-guided deep reinforcement learning of physics-based character skills,” *ACM Transactions On Graphics (TOG)*, vol. 37, no. 4, pp. 1–14, 2018.
- [16] X. B. Peng, E. Coumans, T. Zhang, T.-W. E. Lee, J. Tan, and S. Levine, “Learning agile robotic locomotion skills by imitating animals,” in *Robotics: Science and Systems*, 07 2020.
- [17] J. Wu, J. Wang, and Z. You, “An overview of dynamic parameter identification of robots,” *Robotics and computer-integrated manufacturing*, vol. 26, no. 5, pp. 414–419, 2010.
- [18] X. B. Peng, M. Andrychowicz, W. Zaremba, and P. Abbeel, “Sim-to-real transfer of robotic control with dynamics randomization,” in *2018 IEEE International Conference on Robotics and Automation (ICRA)*. IEEE, 2018, pp. 3803–3810.
- [19] Z. Xie, P. Clary, J. Dao, P. Morais, J. Hurst, and M. Panne, “Learning locomotion skills for cassie: Iterative design and sim-to-real,” in *Conference on Robot Learning*. PMLR, 2020, pp. 317–329.
- [20] T. Wang, R. Liao, J. Ba, and S. Fidler, “Nervenet: Learning structured policy with graph neural networks,” in *International Conference on Learning Representations*, 2018.
- [21] W. Huang, I. Mordatch, and D. Pathak, “One policy to control them all: Shared modular policies for agent-agnostic control,” in *International Conference on Machine Learning*. PMLR, 2020, pp. 4455–4464.
- [22] A. Gupta, L. Fan, S. Ganguli, and L. Fei-Fei, “Metamorph: Learning universal controllers with transformers,” *arXiv preprint arXiv:2203.11931*, 2022.
- [23] C. Yu, W. Zhang, H. Lai, Z. Tian, L. Kneip, and J. Wang, “Multi-embodiment legged robot control as a sequence modeling problem,” in *2023 IEEE International Conference on Robotics and Automation (ICRA)*. IEEE, 2023, pp. 7250–7257.
- [24] B. Trabucco, M. Phielipp, and G. Berseth, “Anymorph: Learning transferable policies by inferring agent morphology,” in *International Conference on Machine Learning*. PMLR, 2022, pp. 21 677–21 691.
- [25] T. Chen, A. Murali, and A. Gupta, “Hardware conditioned policies for multi-robot transfer learning,” *Advances in Neural Information Processing Systems*, vol. 31, 2018.
- [26] W. Yu, J. Tan, C. K. Liu, and G. Turk, “Preparing for the unknown: Learning a universal policy with online system identification,” in *Proceedings of Robotics: Science and Systems*, July 2017.
- [27] A. Kumar, Z. Fu, D. Pathak, and J. Malik, “RMA: Rapid Motor Adaptation for Legged Robots,” in *Proceedings of Robotics: Science and Systems*, July 2021.
- [28] Á. Belmonte-Baeza, J. Lee, G. Valsecchi, and M. Hutter, “Meta reinforcement learning for optimal design of legged robots,” *IEEE Robotics and Automation Letters*, vol. 7, no. 4, pp. 12 134–12 141, 2022.
- [29] C. Finn, P. Abbeel, and S. Levine, “Model-agnostic meta-learning for fast adaptation of deep networks,” in *International Conference on Machine Learning*. PMLR, 2017, pp. 1126–1135.
- [30] K. Cho, B. van Merriënboer, C. Gulcehre, D. Bahdanau, F. Bougares, H. Schwenk, and Y. Bengio, “Learning phrase representations using RNN encoder–decoder for statistical machine translation,” in *Proceedings of the 2014 Conference on Empirical Methods in Natural Language Processing (EMNLP)*. Association for Computational Linguistics, Oct. 2014, pp. 1724–1734.
- [31] J. Vanschoren, “Meta-learning: A survey,” *arXiv preprint arXiv:1810.03548*, 2018.
- [32] J. Beck, R. Vuorio, E. Z. Liu, Z. Xiong, L. Zintgraf, C. Finn, and S. Whiteson, “A survey of meta-reinforcement learning,” *arXiv preprint arXiv:2301.08028*, 2023.
- [33] S. Hochreiter, A. S. Younger, and P. R. Conwell, “Learning to learn using gradient descent,” in *Artificial Neural Networks—ICANN 2001: International Conference Vienna, Austria, August 21–25, 2001 Proceedings 11*. Springer, 2001, pp. 87–94.
- [34] Boston Dynamics, “Spot,” <https://bostondynamics.com/products/spot/>.
- [35] Unitree Robotics, “Aliengo,” <https://www.unitree.com/aliengo/>.
- [36] —, “Go2,” <https://www.unitree.com/go2/>.
- [37] —, “Go1,” <https://www.unitree.com/go1/>.
- [38] —, “B2,” <https://www.unitree.com/b2/>.
- [39] D. Kang, F. De Vincenti, N. C. Adami, and S. Coros, “Animal motions on legged robots using nonlinear model predictive control,” in *2022 IEEE/RSJ International Conference on Intelligent Robots and Systems (IROS)*. IEEE, 2022, pp. 11 955–11 962.
- [40] Y. Shao, Y. Jin, X. Liu, W. He, H. Wang, and W. Yang, “Learning free gait transition for quadruped robots via phase-guided controller,” *IEEE Robotics and Automation Letters*, vol. 7, no. 2, pp. 1230–1237, 2021.
- [41] J. Schulman, F. Wolski, P. Dhariwal, A. Radford, and O. Klimov, “Proximal policy optimization algorithms,” *arXiv preprint arXiv:1707.06347*, 2017.
- [42] J. Schulman, P. Moritz, S. Levine, M. Jordan, and P. Abbeel, “High-dimensional continuous control using generalized advantage estimation,” *arXiv preprint arXiv:1506.02438*, 2015.
- [43] R. Smith *et al.*, “Open dynamics engine,” 2005.
- [44] G. Bleth, M. J. Powell, B. Katz, J. Di Carlo, P. M. Wensing, and S. Kim, “Mit cheetah 3: Design and control of a robust, dynamic quadruped robot,” in *2018 IEEE/RSJ International Conference on Intelligent Robots and Systems (IROS)*. IEEE, 2018, pp. 2245–2252.
- [45] J. Siekmann, S. Valluri, J. Dao, F. Bermillo, H. Duan, A. Fern, and J. Hurst, “Learning Memory-Based Control for Human-Scale Bipedal Locomotion,” in *Proceedings of Robotics: Science and Systems*, July 2020.